Chapter 2

A Room Temperature Methanol Vapor Sensor Based on Highly Conducting Carboxylated Multi-walled Carbon Nanotube/Polyaniline Nanotube Nanocomposite

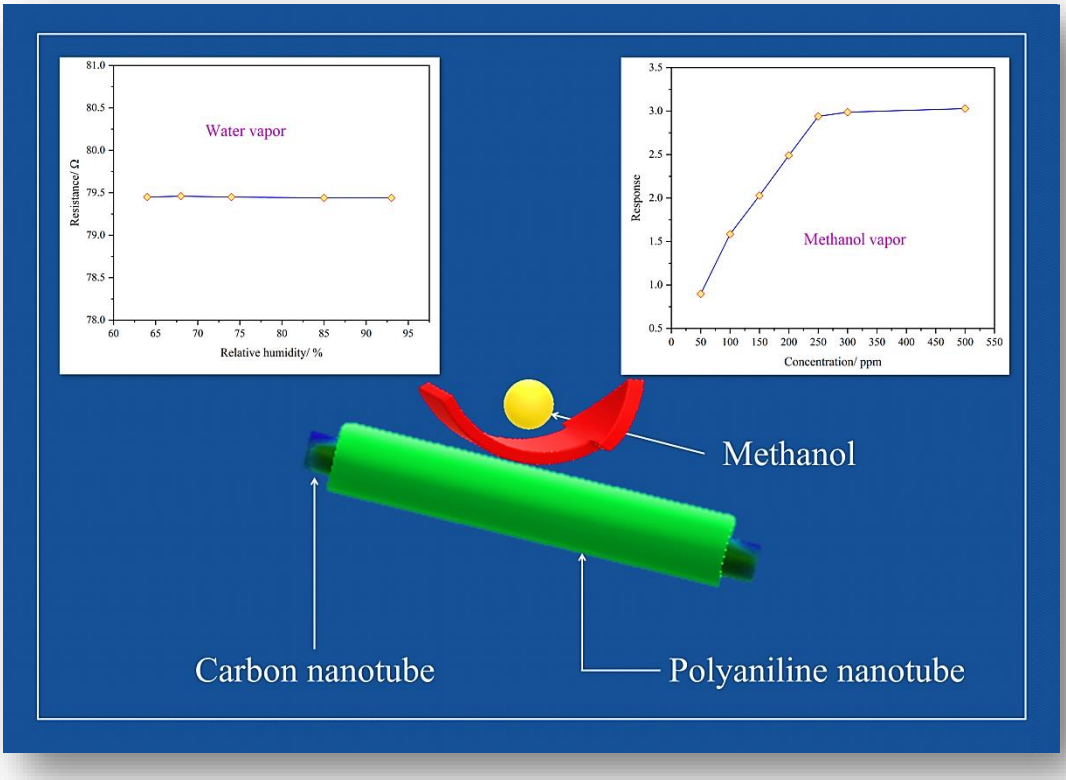

A core shell type carboxylated multi-walled carbon nanotube/polyaniline nanotube nanocomposite is synthesized via *in situ* oxidation polymerization reaction and is applied as a sensing element for detection of methanol vapor.

2.1 Introduction

Since early 1980s, intrinsically conducting polymers (ICPs) such as polyaniline (PAni), polypyrrole (PPy), polythiophene (PTh), polyacetylene (PA), poly(3,4-ethylene-dioxythiophene) (PEDOT) and poly(phenyl vinylene) (PPV) have been exploited as active materials for methanol vapour sensing. These conducting polymers, in comparison to other commercially available sensing elements based on metal oxides, show many advantages like highly reversible redox behavior and can be used at room temperature [1]. Their sensing mechanism is based on their ability to undergo a change in resistance when exposed to vapors. Usually, the vapors get physically or chemically adsorbed on the surface of ICPs and undergo swelling, or they cause redox reactions. Both the processes lead to a change in the electrical resistance of the ICPs which can be correlated with the concentration of methanol vapors present in the environment [2,3]. PAni, in particular, has gained tremendous interest among the ICPs due to its easy doping, good environmental stability and the ability to retain its processing properties [4].

Methanol, a simple aliphatic alcohol, is frequently used as a solvent in paint industries, in chemical and drug industries, in scientific laboratories, as anti-freeze in cars, etc. It comes under the category of volatile organic compounds (VOCs) and the vapors are quite toxic in nature. Acute exposure to these vapors affects the central nervous system (CNS) and causes headache, drowsiness, nausea, loss of vision and even death depending upon the level of exposure. Thus, the monitoring of methanol vapor level at workplaces is very important [5]. Paulraj*et al.* prepared PAni nanoparticles and exposed them to methanol vapors at room temperature. The response signal towards 100 ppm of methanol was the highest for 0.25 M PAni [6]. PAni based sensors, however, faces some limitations such as inferior mechanical stability, insolubility in common solvents, limited detection range and slow response time. Some of the most widely used techniques applied to overcome these limitations are (i) using nanostructured PAni, which provides more active surface area for vapor adsorption and (ii) preparing composites of PAni, that show improved chemical properties and are very sensitive to small

---

This part of the thesis is published in:

Bora, A., Mohan, K., Pegu, D., Gohain, C. B., and Dolui, S. K. A room temperature methanol vapor sensor based on highly conducting carboxylated multi-walled carbon nanotube/polyaniline nanotube composite. *Sensors and Actuators B: Chemical*, 253:977-986, 2017.

changes in the content of filler material [7].Virji*et al.* prepared PAni nanofibers and exposed them to hydrochloric acid, ammonia, hydrazine, chloroform, and methanol. On comparing their sensing behavior to that of conventional PAni films, the nanofibers showed better performance in terms of sensitivity and response time due to their the high surface area and porosity [8].

Adding carbon based nanomaterials like multi-walled carbon nanotubes (MWCNTs) to PAni increases the electrical conductivity of PAni by a few orders of magnitude [9]. MWCNTs have many attractive properties like high electrical conductivity, good chemical stability and morphological flexibility that make them useful as vapor sensors [10]. But a major limitation of MWCNT is its poor selectivity. Combining MWCNTs with PAni provides an ideal approach for fabricating a sensor for vapor sensing. Looking at the literature, composites of PAni and MWCNTs have been widely exploited to sense a number of VOCs like ammonia, chloroform, explosive vapors like picric acid, 2,6-dinitrotoluene (2,6-DNT) and 2,4,6-trinitrotoluene (TNT) and hydrogen gas [11–14].

Alan G. MacDiarmid, one of three recipients of the Nobel Prize for chemistry in 2000 has once famously said that *"There are as many different types of polyaniline as there are people who synthesize it"* [15]. Literature study reveals that the conductivity of individual polyaniline nanotubes (PAniNT) is significantly high [16]. PAniNT is considered as a one-dimensional nanostructure (ODNS) and thus has a longer polymer conjugated backbone compared to other morphologies, which can result in increased conductivity and higher mobility [17,18].

In this work, we report the template free synthesis of PAniNT, and its nanocomposite formation with different weight percentages (wt%) of carboxylated MWCNTs (c-MWCNTs) *viain situ* chemical oxidation polymerization technique. A unique core-shell morphology is observed where the c-MWCNT acts as a core around which a shell of PAniNT is formed. The structural, electrical and electrochemical properties of the nanocomposites with variation of c-MWCNT content are elaborately investigated. The responsive behavior of these c-MWCNT/PAniNT nanocomposites on exposure to methanol vapors of different concentrations as well as ethanol and propanol vapors are also investigated using a two probe configuration. In addition, the repeatability and the stability of the sensing element are examined over a one month period. Moreover, the experimental results are correlated with theoretical calculations using density functional theory (DFT).

2.2 Materials and methods

2.2.1 Chemicals

Aniline, ammonium peroxydisulphate (APS), methanol, acetic acid, concentrated nitric

acid and concentrated sulphuric acid purchased from Merck were analytical reagent grade chemicals and used as received. MWCNT was purchased from Redex Technologies Private Limited. Ethanol and propanol were obtained from Changshu Yanguan Chemical Company and Rankem respectively. For all purposes, double distilled water was used.

2.2.2 Synthesis

2.2.2.1 Preparation of PAniNT.PAniNTs were prepared according to the procedure applied by Huang *et al.* [19]. In a typical synthesis procedure, two separate solutions of aniline monomer and oxidant APS were prepared in an aqueous reaction medium of 0.4 M acetic acid and 1 M methanol in distilled water. Both the solutions were cooled at 0-5 °C for 30 min, and then mixed and stirred vigorously for 30 s. The mixture was left undisturbed overnight at 0-5 °C to obtain maximum precipitation. The precipitate was washed with distilled water and finally dried in vacuum overnight to obtain PAniNT.

2.2.2.2 Carboxylation of pristine MWCNTs.MWCNTs were carboxylated according to the procedure followed by Datsyuk*et al.*[20]. In the functionalization reaction, a 100 mL round bottom flask was fitted with a condenser. 0.3 g of MWCNTs was dispersed in 25 mL of nitric acid in the flask. The dispersion was refluxed at 85 °C under magnetic stirring for 48 h. The resulting dispersion was diluted with water and washed repeatedly until neutral pH was obtained. The powder was dried in vacuum overnight at 40 °C to obtain c-MWCNTs.

2.2.2.3 Preparation of c-MWCNT/PAniNT nanocomposites.The c-MWCNT/PAniNT nanocomposites with different content of c-MWCNTs ranging from 1-7 wt% were synthesized by *in situ* chemical oxidation polymerization of aniline in presence of c-MWCNTs. Different quantities of c-MWCNTs (1, 3, 4, 5, 6 and 7 wt%) were ultrasonicated in distilled water for 3 h to obtain properly dispersed suspensions. Two reaction solutions of aniline and APS were prepared according to the previously mentioned method of PAniNT synthesis. All the three solutions were cooled at 0-5 °C for 30 min, and then mixed and stirred vigorously for 30 s. The mixture was allowed to react undisturbed overnight at 0-5 °C. The products were washed with distilled water and ultimately dried in vacuum overnight to obtain c-MWCNT/PAniNT nanocomposites.

2.2.3 Characterization

2.2.3.1 Instruments.A Nicolet Impact-410 IR spectrometer was used to record the Fourier transform infra-red (FTIR) spectra of the samples in the range of 400-4000 cm^{-1}. A Shimadzu UV-2550 spectrophotometer was used to record the electronic absorption spectra of

the samples. A MiniflexRigaku Japan was used to collect the X-ray diffraction (XRD) pattern of the samples by using CuKα radiation (λ = 0.15418 nm) in 10–70 degree range. A JEOL JEM 2100 (200 kV) was used to obtain transmission electron microscope (TEM) micrographs. Four probe technique was used to measure the conductivities of the samples, and a Keithley 2400 source meter was used to study current-voltage (*I*–*V*) relationship.

2.2.3.2 Set-up for vapor sensing. A simple two probe configuration was used as a set-up for sensing the response behavior of the nanocomposites towards alcohol vapors at room temperature **(Figure 2.1)**. The samples were made into 0.2 cm thick pellets by uniaxial pressing under a pressure of 6.9 bar. The pellet was then fixed to the contact leads by using silver paste and exposed to alcohol vapors of different concentrations ranging from 50 ppm to 500 ppm in a closed environment. The sensing element was hanged 2 cm above the solution surface and the change in resistance of the pallets before and after exposure was recorded with a Keithley 2400 source meter. Distilled water was used to prepare the alcohol solutions.

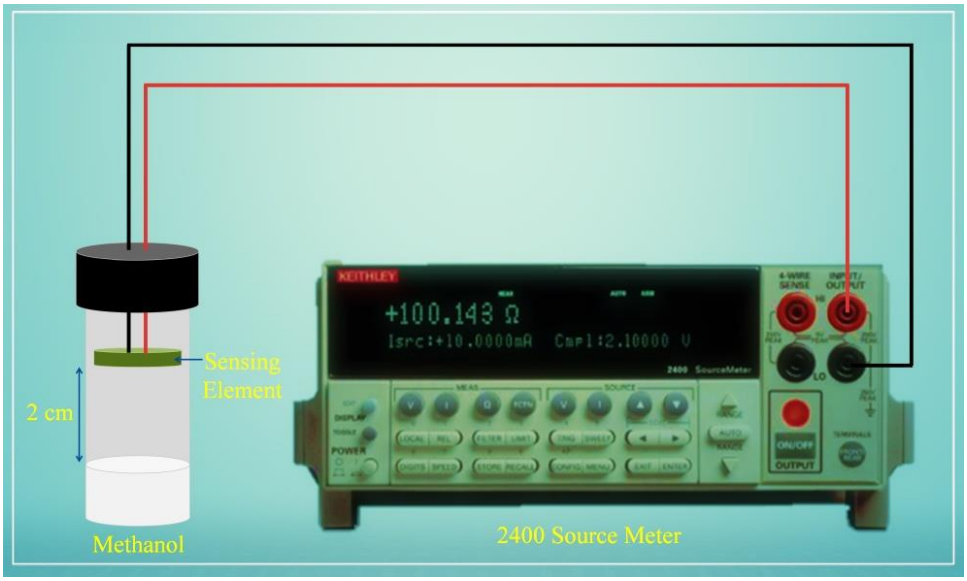

Figure 2.1 Configuration for measuring resistance on exposure to methanol vapor.

2.3 Results and Discussion

2.3.1 FTIR spectra analyses. The FTIR spectra of PAniNT, c-MWCNTs and 6 wt% c-MWCNT/PAniNT nanocomposite are shown in **Figure 2.2**. For PAniNT, a broad vibration band at 3421 cm^{-1} appears due to N-H stretching while the bands at 1573 cm^{-1} and 1492 cm^{-1} appear due to C=C stretching of quinoid and benzoid ring respectively [21,22]. The bands at 1304 cm^{-1}, 1249 cm^{-1}, 1113 cm^{-1} and 812 cm^{-1} represents C-N stretching, C–N–C stretching, N-Q-N vibration and asymmetric 1,4-disubstituted benzoid ring vibrations respectively. According to

Trchova*et al.*, at pH above 4 aniline monomers and oligomers can undergo electrophilic attack of sulfonation [23]. This effect can be observed in the appearance of bands at 1031 cm^{-1} and 605 cm^{-1} due to S=O and S–C stretching vibration modes respectively. Carboxylation of MWCNTs is confirmed in the FTIR spectrum of c-MWCNTs by the appearance of the peaks at 3430 cm^{-1}, 1735 cm^{-1}, 1632 cm^{-1} and 1024 cm^{-1} due to stretching vibrations of -COOH [24,25]. The bands at 2926 cm^{-1} and 1445 cm^{-1} are attributed to C–H stretching and hydrogen bonds respectively. From the FTIR spectrum of 6 wt% c-MWCNT/PAniNT, it is evident that the functional identities of the individual components remain intact, although the intensities of the bands are affected. The decrease in the intensity of bands of the nanocomposites in comparison to the PAniNT could be attributed to the possible restriction to the vibrational bonds in PAniNT. This generally occurs when Ani monomers are adsorbed on the c-MWCNTs and their growth is constrained during the polymerization reaction.

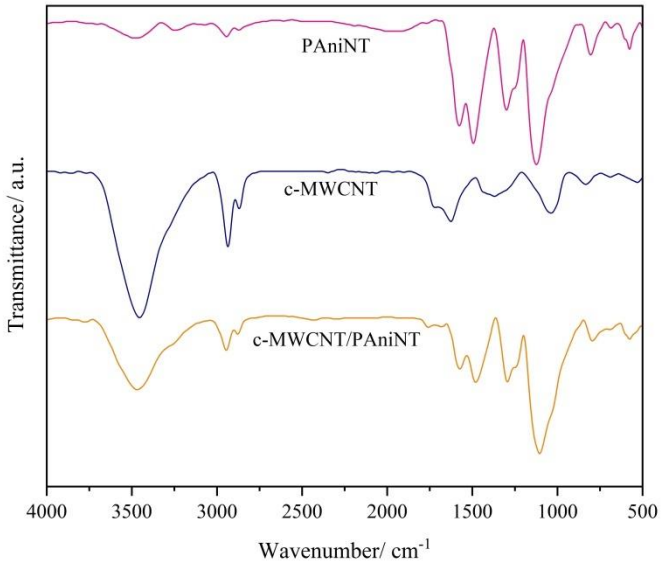

Figure 2.2 FTIR spectra of PAniNT, c-MWCNT and 6 wt% c-MWCNT/PAniNT.

2.3.2 Ultraviolet-visible (UV-vis) spectra analyses. The UV-vis spectra of PAniNT, c-MWCNTs and 6 wt% c-MWCNT/PAniNT are shown in **Figure 2.3**. Two characteristic peaks appear at 325 nm and 633 nm in the spectrum of PAniNT corresponding toπ-π* transitions within the benzoid ring and the quinoid ring of PAni respectively [26]. In case of c-MWCNTs, a single peak appears at 258 nm due to π plasmon absorbance. For 6 wt% c-MWCNT/PAniNT three peaks appear, two of which are indicative of PAniNT and one represents c-MWCNTs. These peaks are affirmative of effective interaction between the individual components [27].

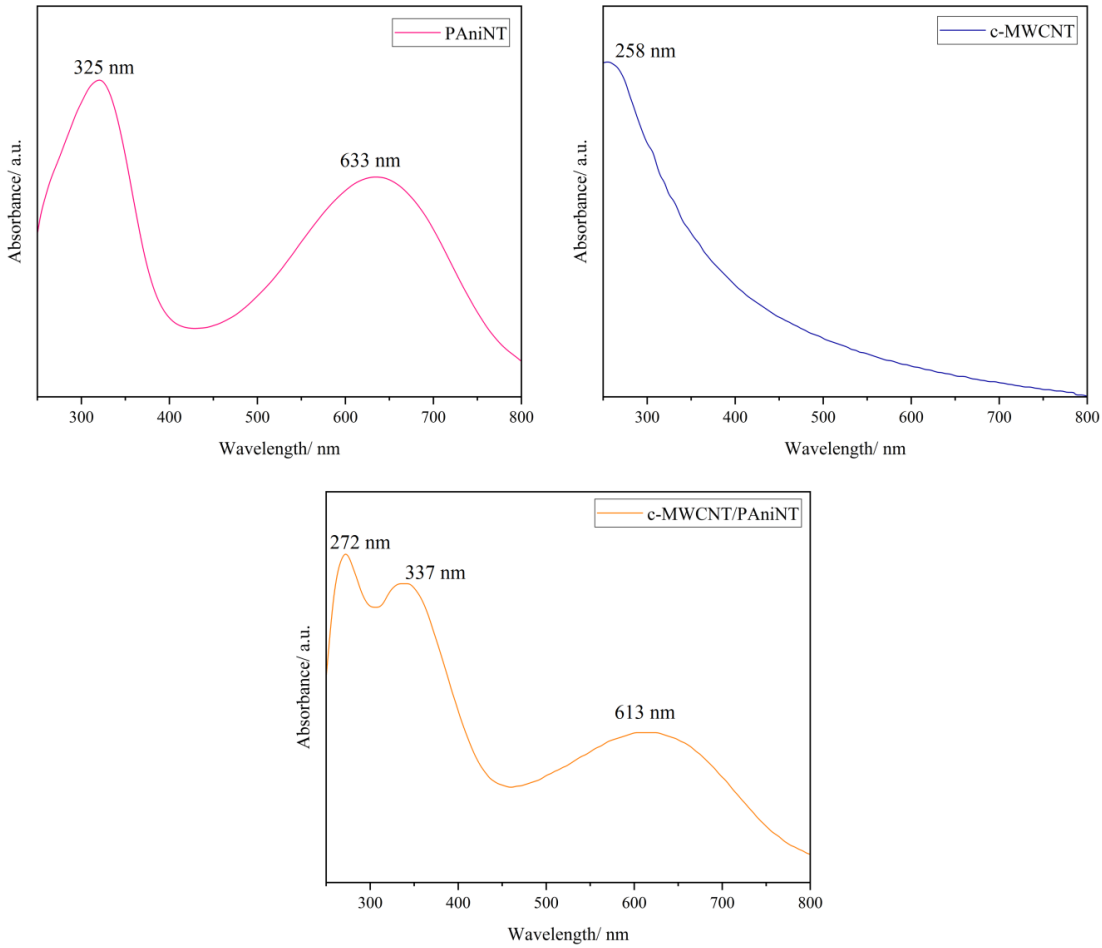

Figure 2.3 UV-vis spectra of PAniNT, c-MWCNT and 6 wt% c-MWCNT/PAniNT.

2.3.3 XRD analyses. The XRD peaks of PAniNT, c-MWCNTs and c-MWCNT/PAniNT are shown in **Figure 2.4**. In case of PAniNT, diffraction peaks appear at 2θ = 16.0º, 18.4º and

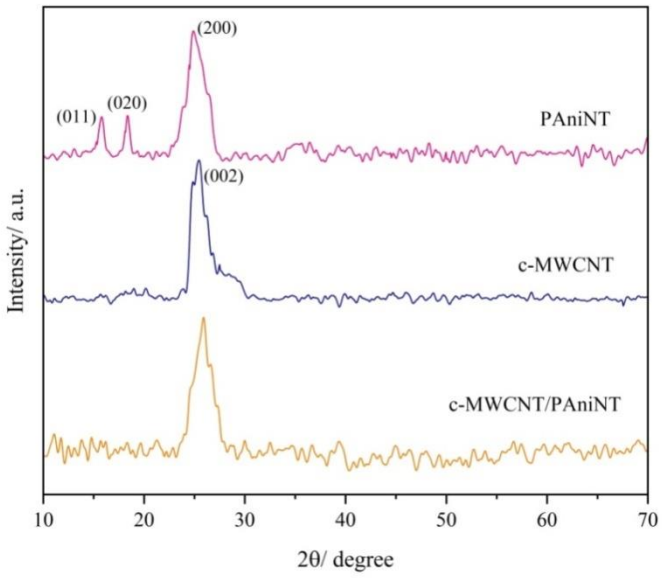

Figure 2.4 XRD patterns of PAniNT, c-MWCNT and 6 wt% c-MWCNT/PAniNT.

24.9º corresponding to (011), (020) and (200) crystal planes of PAni [28]. For c-MWCNTs, a sharp peak is observed at 2θ = 25.4º corresponding to (002) plane [29]. This peak indicates the graphite-like structure of MWCNTs. When c-MWCNTs are incorporated into PAniNT, the peaks at 2θ = 25.8º for both PAniNT and c-MWCNTs overlap. Both PAniNT and c-MWCNTs are semi-crystalline in nature and no new crystalline nature appears due to their interaction in the nanocomposite.

2.3.4 Morphological studies.The TEM micrograph of PAniNT shows that it appears in tubular morphology **(Figure 2.5 (a))**. One-dimensional growth of PAniNT is promoted by the hydrogen bonding between methanol molecules. These interactions are perpendicular to the PAni chains which push them apart [30]. Acetic acid, on the other hand, brings down the pH of the reaction. Both these parameters cause a synergetic effect and lead to the growth of PAniNT. The mean diameter of the PAniNT is 200 nm. Carboxylation of pristine MWCNTs leads to shortening of MWCNTs. The outer diameter of the c-MWCNTs varies in the range from 20-25 nm **(Figure 2.5 (b))**. In the TEM micrographs of 6 wt% c-MWCNT/PAniNT, a co-axial core-shell type of morphology is seen **(Figure 2.5 (c))** [31]. The inner core consists of c-MWCNT with an average outer diameter of 20-25 nm, which matches with the results obtained for c-MWCNT. The PAniNT grows around its outer surface in a uniform manner, acting as a shell. The overall diameter of the c-MWCNT/PAniNT composite is 70-80 nm. It is interesting to note that without any support, the pristine PAniNT has a larger diameter but with c-MWCNT acting as a support, the diameter of the c-MWCNT/PAniNT composite reduces. It can be postulated that the aniline monomer first gets adsorbed on the surface of the c-MWCNT followed by polymerization during the course of the reaction, leading to uniform tubular growth. Functional groups like –COOH are generated when pristine MWCNTs are treated with nitric acid. They lead to formation of hydrogen bonds between c-MWCNTs, and the nitrogen of benzenoid and quinoid

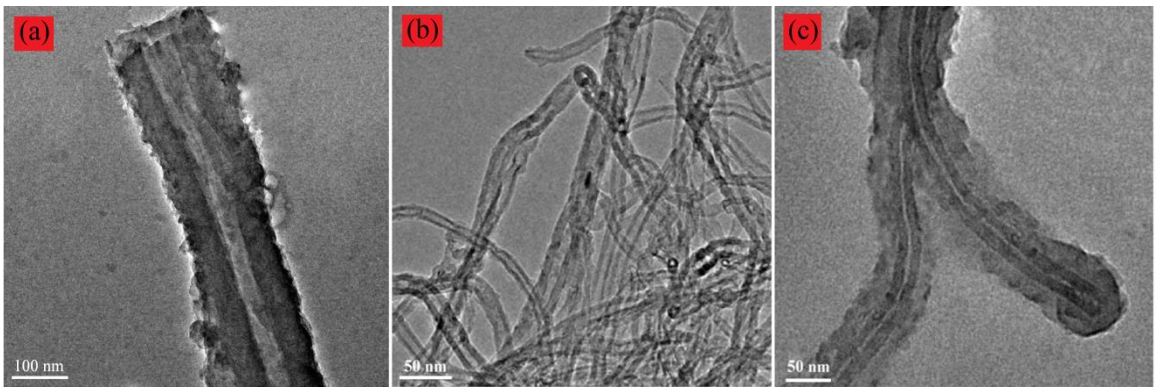

Figure 2.5 TEM micrographs of **(a)** PAniNT, **(b)** c-MWCNT and **(c)** 6 wt% c-MWCNT/PAniNT.

groups of PAniNT. Another type of interaction that takes place is π-π stacking between aromatic rings of PAniNT and the c-MWCNTs [31]. The schematic representation of the interactions between PAni chains and c-MWCNTs is presented in **Scheme 2.1**.

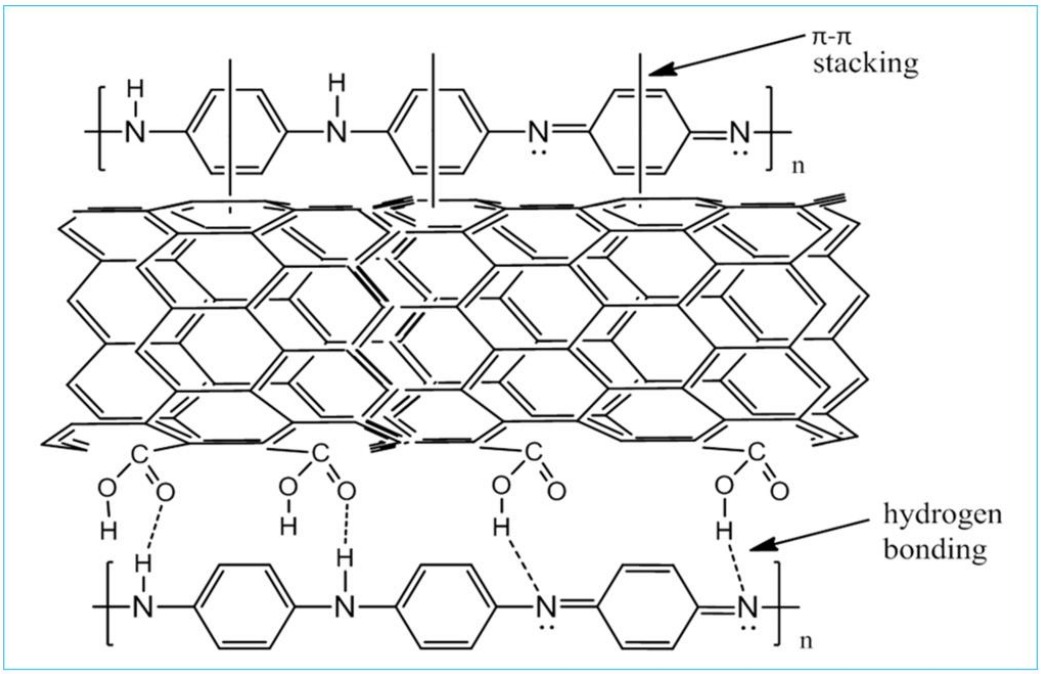

Scheme 2.1 Schematic representation of the interactions between PAniNT and c-MWCNTs.

2.3.5 DC electrical conductivities. The DC electrical conductivities of PAniNT and c-MWCNT/PAniNT composites as a function of varying c-MWCNT content are given in **Table 2.1**. Initially, the conductivity of pristine PAniNT is 0.028 Scm^{-1}. With the incorporation of c-MWCNT, the conductivity starts to increase, reaches a maximum of 6.15 Scm^{-1} at 6 wt% c-MWCNT and then gradually decreases with further increase in c-MWCNT content. PAni chains are believed to act as bridged linkages and offer conductive paths on the surface of c-MWCNTs that enables easier charge transfer between the two. This effect leads to a dramatic increase in the conductivity of c-MWCNT/PAniNT. Furthermore, effective site-selective interactions between the quinoid rings of PAni and MWCNTs have also been reported which also enhance the charge-transfer processes [32]. But with further increase in c-MWCNT content, the influence of the PAniNT chains as bridged linkages decreases and a decrease in the conductivity of the nanocomposites is seen.

Table 2.1 DC electrical conductivities of PAniNT and c-MWCNT/PAniNT nanocomposites with varying c-MWCNT content.

Material	c-MWCNT content/ wt%	Resistivity/ Ω cm	Conductivity/ Scm^{-1}
PAniNT	0	35.714	0.028
c-MWCNT/PAniNT	1	7.936	0.126
c-MWCNT/PAniNT	3	0.698	1.432
c-MWCNT/PAniNT	4	0.521	1.920
c-MWCNT/PAniNT	5	0.254	3.929
c-MWCNT/PAniNT	6	0.162	6.154
c-MWCNT/PAniNT	7	0.298	3.349

2.3.6 Vapor sensing study. We monitored the sensing response of 6 wt% c-MWCNT/PAni nanocomposite towards methanol vapor at room temperature. Initially, the nanocomposite is exposed to water vapor in a closed environment with relative humidity (R_H) in the range 65% to 95% at 25 ºC **(Figure 2.6 (a))**. No change in the resistance of the material is observed even after 10 min of exposure indicating its non-responsive nature towards water vapor. However, when it is exposed to methanol vapor, an increase in its resistance is observed. This increase can be correlated with the sensor response (S) according to **relation (2.1).**

$$S = \frac{R_{(after\ exposure)} - R_{(before\ exposure)}}{R_{(before\ exposure)}} \qquad \textbf{(2.1)}$$

where$R$ is resistance. Methanol solutions of different concentrations were prepared by mixing methanol and distilled water in different volume ratios. We measured the R_H of the sensing chamber at 25 ºC in presence of the aforementioned methanol concentrations with the help of a hygrometer and found a steady decrease from 83% to 69% with increasing concentration**(Figure 2.6 (b))**. The pellet was then placed inside the sensing chamber. On monitoring the response with increasing concentration, a gradual increase in the sensor response is seen which reaches a saturation point after 250 ppm concentration **(Figure 2.6 (b))**.

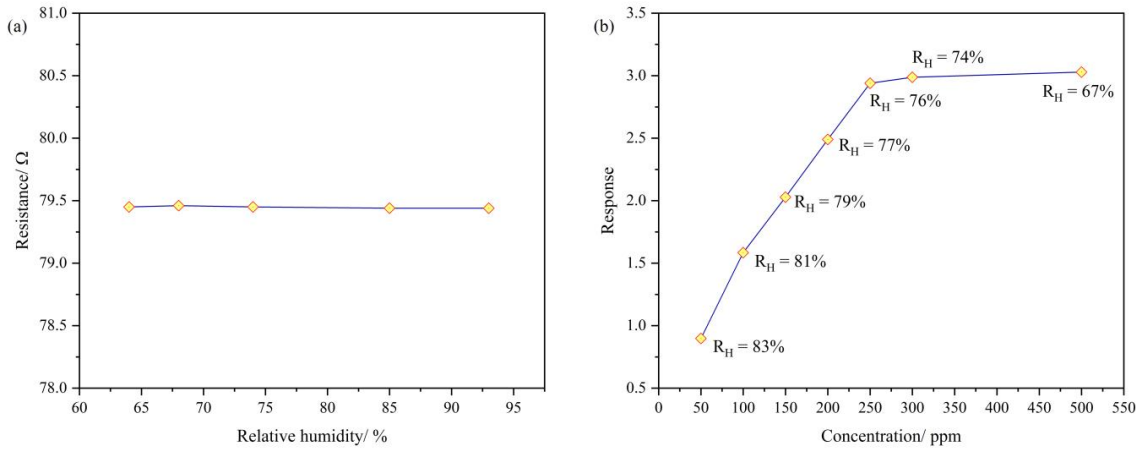

Figure 2.6 Response of 6 wt% c-MWCNT/PAniNT towards **(a)** water vapor and **(b)** methanol vapor.

The responsive behavior is driven by the disruption of old hydrogen bonds between PAniNT and c-MWCNTs, and formation of new hydrogen bonds between methanol molecules and both PAniNT and c-MWCNTs **(Scheme 2.2)**. The new bonds push the PAni chains away from planarity, which causes a decrease in delocalization of polarons and bipolarons. Additionally, when $R_H$is comparatively low, more effective sites for hydrogen bonding to methanol molecules are available. Since in the same R_H range, exposure to water vapor showed no response, we can conclude that the sensor response is due to methanol vapor only.

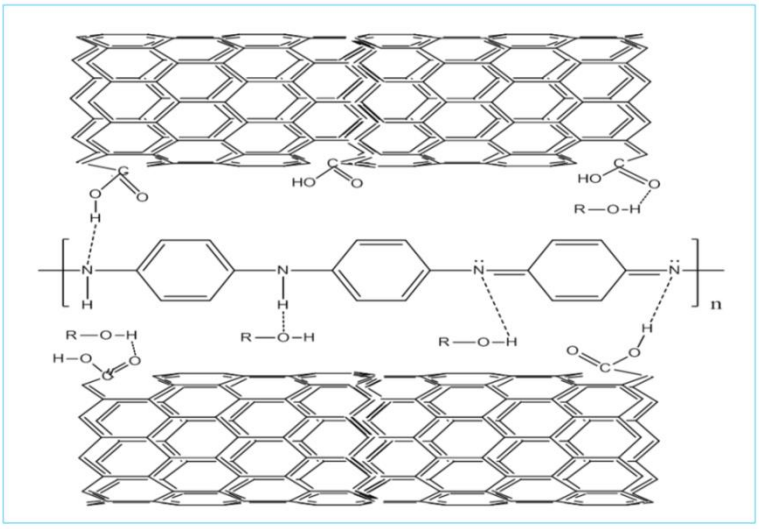

Scheme 2.2 Schematic representation of the interactions between methanol and c-MWCNT/PAniNT.

We also investigated the response of pristine PAniNT and 1 wt% c-MWCNT/PAniNT towards methanol **(Figure 2.7)**. It is observed that the response shown by pristine PAniNT is the lowest while that of 1 wt% c-MWCNT/PAniNT is higher than it but still lower than 6 wt% c-

MWCNT/PAniNT. This result establishes that fact that sensor response has a proportional relationship with the conductivity of the sensing element.

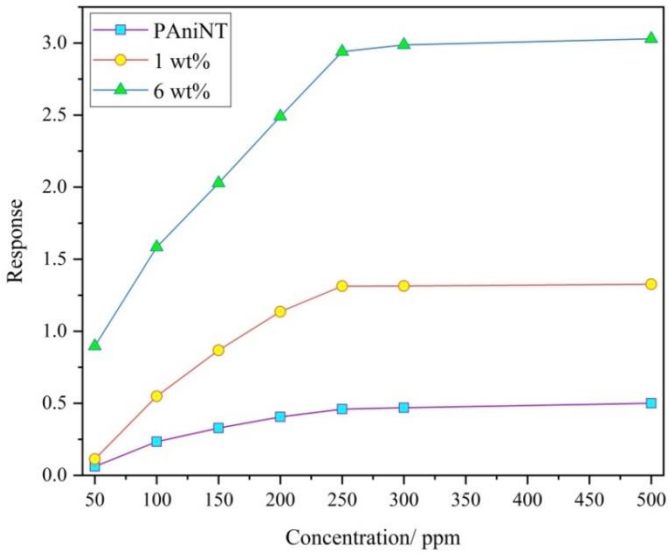

Figure 2.7 Response of PAniNT, 1 wt% c-MWCNT/PAniNT and 6 wt% c-MWCNT/PAniNT towards methanol vapor of different concentrations.

The recovery time of the sensing element was obtained by blowing hot air of temperature above the boiling point of methanol, and then allowing it to cool to room temperature. The recovery time obtained is 90 s, which is slightly longer than its response time of 60 s. But interestingly, there is full recovery of the sensing element. Furthermore, when it is subjected to continuous "on-off" cycles of methanol exposure of 80 ppm concentration, the activity of the sensing element remains unaffected upto about 10 cycles **(Figure 2.8 (a))**. It also remains effective for about 20 days after which the response starts to decrease **(Figure 2.8 (b))**. This might be due to degradation of the nanocomposite over time.

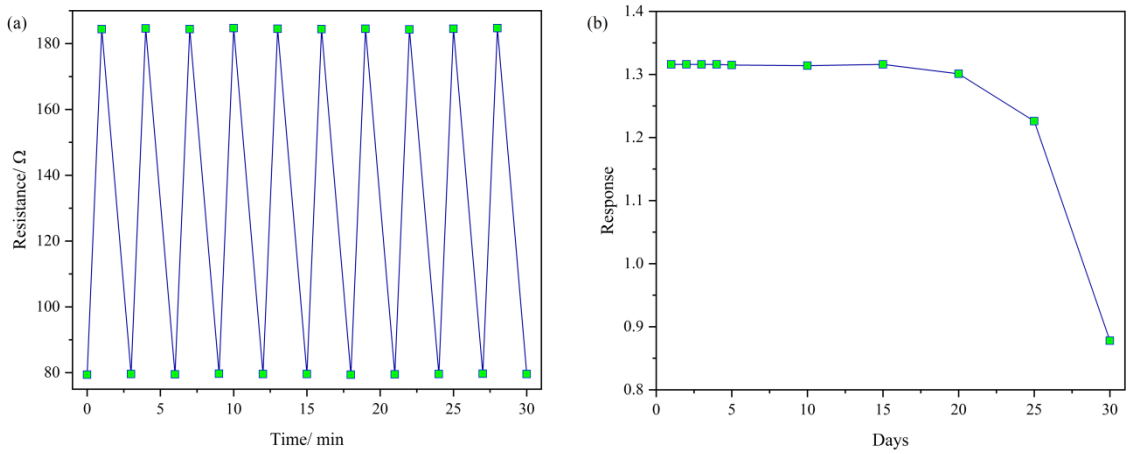

Figure 2.8(a) Repeatability and **(b)** stability tests of 6 wt% c-MWCNT/PAniNT.

We compared the response of 6 wt% c-MWCNT/PAniNT towards ethanol and propanol vapor with that of methanol vapor. It is seen from **Figure 2.9** that the response is the highest for methanol vapor followed by ethanol and propanol. This observation can be explained on the basis of polarity and size effects [33]. The polarity of the alcohols decreases with growing chain length. Also, higher alcohols, due to their bigger size might find it difficult to reach the active sites of the nanocomposite but methanol can easily bind to their surface. These two effects manifest in the lower sensitivity of the nanocomposite towards higher alcohols.

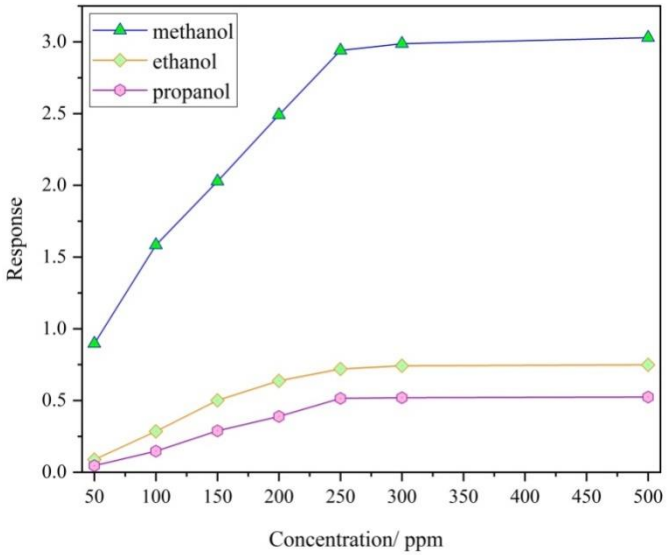

Figure 2.9 Response of 6 wt% c-MWCNT/PAniNT towards methanol, ethanol and propanol vapors of different concentrations.

2.3.6 DFT study. Theoretical information on the formation of hydrogen bonded molecules can be obtained from DFT calculations based on generalized gradient approximation (GGA) [34]. Experimental results show that a change in resistance of PAni on exposure to methanol vapors is most likely due to hydrogen bonding between them. We employed DFT with basis set *B3LYP/6-31+G** to verify our results as tabulated in **Table 2.2**. These results confirm hydrogen bond formation between PAni chains and alcohol molecules **(Figure 2.10)**. With higher alcohols, increase in bond length and binding energy is seen, thus confirming their weak response towards the sensing element. In addition, the change in the dihedral angles also ratifies the loss in planarity of the PAniNT chain on interaction with alcohols.

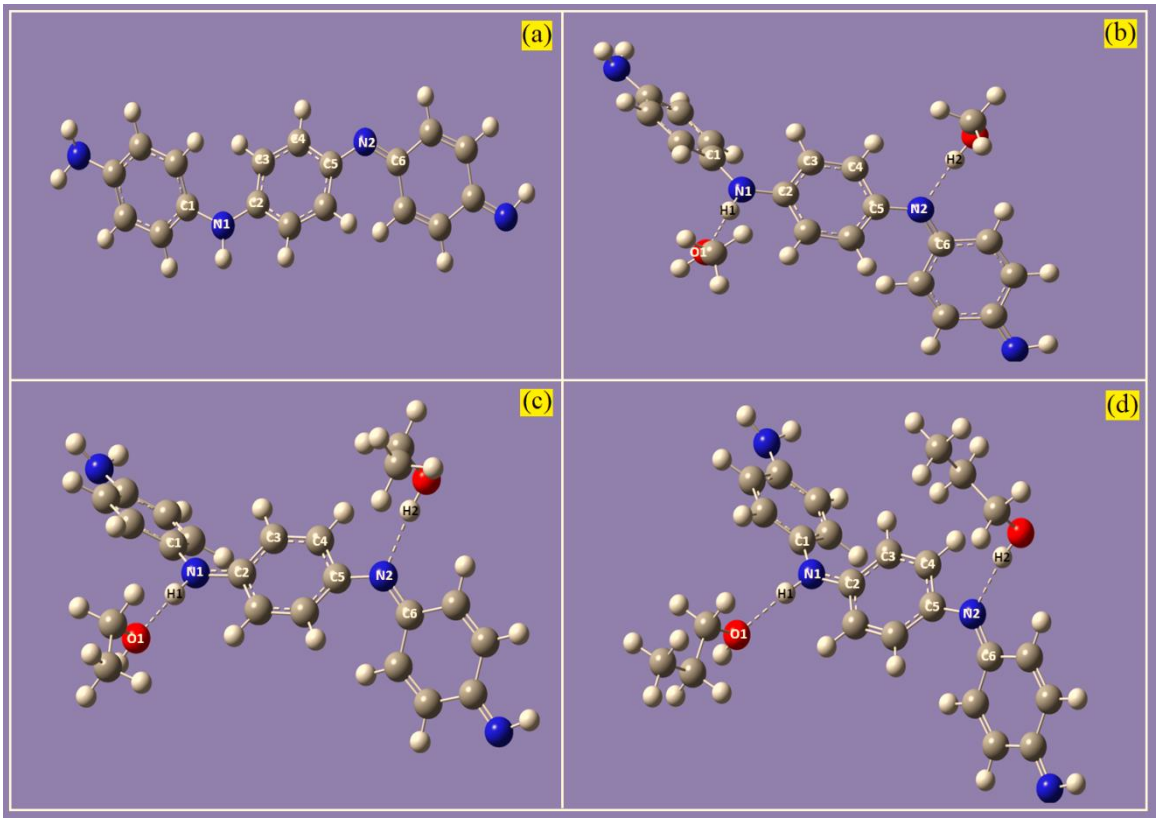

Figure 2.10 DFT studies of **(a)** PAniNT, and interactions of PAniNT with **(b)** methanol, **(c)** ethanol and **(d)** propanol.

Table 2.2 DFT parameters calculated during interaction of PAni with methanol, ethanol and propanol.

System	Hydrogen bond length/ nm		Dihedral angle/ degree		Binding energy/ kCal mol^{-1}
	O1-H1	N2-H2	C1-N1-C2	C5-N2-C6	
PAni	-	-	-10.8	-146.7	-
PAni-methanol	0.200138	0.191900	13.2	-147.9	15.94
PAni-ethanol	0.200178	0.194537	12.7	-147.8	26.04
PAni-propanol	0.200189	0.194872	13.1	-147.1	34.70

2.4 Conclusion

PAniNT and c-MWCNT/PAniNT nanocomposites have been successfully prepared and characterized. TEM micrographs indicate that c-MWCNTs/PAniNT exists in core-shell structure. For the nanocomposites, the electrical conductivity increases with increasing c-MWCNT amount upto 6 wt%. PAniNT and its composites have been tested as alcohol sensing elements and the 6 wt% c-MWCNT/PAniNT nanocomposite exhibits the highest response towards methanol vapor at concentration as low as 50 ppm. The change in resistance of the sensing element upon exposure to alcohol vapors is caused by hydrogen bond formation between the methanol molecules and the conjugated PAni chains, which is confirmed by DFT studies. The nanocomposite shows a below average response for ethanol while for propanol, the response is very poor. So it can be concluded that 6 wt% c-MWCNT/PAniNT nanocomposite is a potential sensing material for detecting methanol vapor.

2.5 References

[1] Bai, H. and Shi, G. Gas sensors based on conducting polymers. *Sensors*, 7(3):267-307, 2007.

[2] Konwer, S., Guha, A. K., and Dolui, S. K. Graphene oxide-filled conducting polyaniline composites as methanol-sensing materials. *Journal of Materials Science*, 48(4):1729-1739, 2013.

[3] Das, D., Choudhury, P., Borthakur, L. J., Kamrupi, I. R., Gogoi, U., and Dolui, S. K. Methanol vapor sensor based on poly(styrene-co-butylacrylate)/polypyrrole-EG core–shell nanocomposites. *Sensors and Actuators B: Chemical*, 199:320-329, 2014.

[4] Nicolas-Debarnot, D. and Poncin-Epaillard, F. Polyaniline as a new sensitive layer for gas sensors. *Analytica Chimica Acta*, 475:1-15, 2003.

[5] Kavet, R. and Nauss, K. M. The toxicity of inhaled methanol vapors. *Critical Reviews in Toxicology*, 21(1):21-50, 1990.

[6] Paulraj, R., Mani, G. K., Nallathambi, L., and Rayappan, J. B. B. A room temperature methanol vapour sensor based on polyaniline nanoparticles. *Journal of Nanoscience and Nanotechnology*, 16(8):8315-8321, 2016.

[7] Hatchett, D. W. and Josowicz, M. Composites of intrinsically conducting polymers as sensing nanomaterials. *Chemical Reviews*, 108(2):746-769, 2008.

[8] Virji, S., Huang, J., Kaner, R. B., and Weiller, B. H. Polyaniline nanofiber gas sensors: Examination of response mechanisms. *Nano Letters*, 4(3):491-496, 2004.

[9] Kondawar, S. B., Deshpande, M. D., and Agrawal, S. P. Transport properties of conductive polyaniline nanocomposites based on carbon nanotubes. *International Journal of Composite Materials*, 2(3):32-36, 2012.

[10] An, K. H., Jeong, S. Y., Hwang, H. R., and Lee, Y. H. Enhanced sensitivity of a gas sensor incorporating single-walled carbon nanotube-polypyrrole nanocomposites. *Advanced Materials*, 16(12):1005-1009, 2004.

[11] Yoo, K.-P., Kwon, K.-H., Min, N.-K., Lee, M. J., and Lee, C. J. Effects of O_2 plasma treatment on NH_3 sensing characteristics of multiwall carbon nanotube/polyaniline composite films. *Sensors and Actuators B: Chemical*, 143(1):333-340, 2009.

[12] Kar, P. and Choudhury, A. Carboxylic acid functionalized multi-walled carbon nanotube doped polyaniline for chloroform sensors. *Sensors and Actuators, B: Chemical*, 183:25-33, 2013.

[13] Yuan, C.-L., Chang, C.-P., Hong, Y.-S., and Sung, Y. Fabrication of MWNTs – PANI composite – A chemiresistive sensor material for the detection of explosive gases. *Materials Science-Poland*, 27(2):509-520, 2009.

[14] Srivastava, S., Sharma, S. S., Kumar, S., Agrawal, S., Singh, M., and Vijay, Y. K. Characterization of gas sensing behavior of multi walled carbon nanotube polyaniline composite films. *International Journal of Hydrogen Energy*, 34(19):8444-8450, 2009.

[15] MacDiarmid, A. G. Preface. In Zarras P, Stenger-Smith JD, and Wei Y, eds., editors, *Electroactive Polymers for Corrosion Control*, pages xi-xvi, ISBN:9780841219465. American Chemical Society, Washington, DC, 2003.

[16] Long, Y., Zhang, L., Ma, Y., Chen, Z., Wang, N., Zhang, Z., and Wan, M. Electrical conductivity of an individual polyaniline nanotube synthesized by a self-assembly method. *Macromolecular Rapid Communications*, 24(16):938-942, 2003.

[17] Kuchibhatla, S. V. N. T., Karakoti, A. S., Bera, D., and Seal, S. One dimensional nanostructured materials. *Progress in Materials Science*, 52(5):699-913, 2007.

[18] Weng, B., Liu, S., Tang, Z.-R., and Xu, Y.-J. One-dimensional nanostructure based materials for versatile photocatalytic applications. *RSC Advances*, 4(25):12685-12700, 2014.

[19] Huang, Z., Liu, E., Shen, H., Xiang, X., Tian, Y., Xiao, C., and Mao, Z. Preparation of polyaniline nanotubes by a template-free self-assembly method. *Materials Letters*, 65(13):2015-2018, 2011.

[20] Datsyuk, V., Kalyva, M., Papagelis, K., Parthenios, J., Tasis, D., Siokou, A., Kallitsis, I., and Galiotis, C. Chemical oxidation of multiwalled carbon nanotubes. *Carbon*, 46(6):833-840, 2008.

[21] Butoi, B., Groza, A., Dinca, P., Balan, A., and Barna, V. Morphological and structural analysis of polyaniline and poly(o-anisidine) layers generated in a DC glow discharge plasma by using an oblique angle electrode deposition configuration. *Polymers*, 9(12):732, 2017.

[22] Du, X., Xu, Y., Xiong, L., Bai, Y., Zhu, J., and Mao, S. Polyaniline with high crystallinity degree: Synthesis, structure, and electrochemical properties. *Journal of Applied Polymer Science*, 131(19):40827, 2014.

[23] Trchová, M., Šeděnková, I., Konyushenko, E. N., Stejskal, J., and Ćirić-Marjanović, G. Evolution of polyaniline nanotubes: The oxidation of aniline in water. *The Journal of Physical Chemistry B*, 110(19):9461-9468, 2006.

[24] Zhang, F., Weidmann, A., Nebe, J. B., and Burkel, E. Osteoblast cell response to surface-modified carbon nanotubes. *Materials Science and Engineering C*, 32(5):1057-1061, 2012.

[25] Park, O.-K., Jeevananda, T., Kim, N. H., Kim, S., and Lee, J. H. Effects of surface modification on the dispersion and electrical conductivity of carbon nanotube/polyaniline composites. *Scripta Materialia*, 60(7):551-554, 2009.

[26] Vaghela, C., Kulkarni, M., Karve, M., Aiyer, R., and Haram, S. Agarose-guar gum assisted synthesis of processable polyaniline composite: Morphology and electro-responsive characteristics. *RSC Advances*, 4(104):59716-59725, 2014.

[27] Sainz, R., Benito, A. M., Martínez, M. T., Galindo, J. F., Sotres, J., Baró, A. M., Corraze, B., Chauvet, O., and Maser, W. K. Soluble self-aligned carbon nanotube/polyaniline composites. *Advanced Materials*, 17(3):278-281, 2005.

[28] Ding, L., Li, Q., Zhou, D., Cui, H., An, H., and Zhai, J. Modification of glassy carbon electrode with polyaniline/multi-walled carbon nanotubes composite: Application to electro-reduction of bromate. *Journal of Electroanalytical Chemistry*, 668:44-50, 2012.

[29] Zhao, T., Hou, C., Zhang, H., Zhu, R., She, S., Wang, J., Li, T., Liu, Z., and Wei, B. Electromagnetic wave absorbing properties of amorphous carbon nanotubes. *Scientific Reports*, 4(1):5619, 2014.

[30] Zhou, S., Wu, T., and Kan, J. Effect of methanol on morphology of polyaniline. *European Polymer Journal*, 43(2):395-402, 2007.

[31] Ramana, G. V., Srikanth, V. V. S. S., Padya, B., and Jain, P. K. Carbon nanotube-polyaniline nanotube core-shell structures for electrochemical applications. *European Polymer Journal*, 57:137-142, 2014.

[32] Cochet, M., Maser, W. K., Benito, A. M., Callejas, M. A., Martínez, M. T., Benoit, J. M., Schreiber, J., and Chauvet, O. Synthesis of a new polyaniline/nanotube composite: "In-situ" polymerisation and charge transfer through site-selective interaction. *Chemical Communications*, 0(16):1450-1451, 2001.

[33] Kar, P., Pradhan, N. C., and Adhikari, B. Application of sulfuric acid doped poly (m-aminophenol) as aliphatic alcohol vapor sensor material. *Sensors and Actuators, B: Chemical*, 140(2):525-531, 2009.

[34] Ullah, H., Shah, A. U. H. A., Bilal, S., and Ayub, K. DFT study of polyaniline NH_3, CO_2, and CO gas sensors: Comparison with recent experimental data. *The Journal of Physical Chemistry C*, 117(45):23701-23711, 2013.